ORNLMIT231

NTIS
One Source. One Search. One Solution.

GAS-LIQUID MASS TRANSFER IN A THREE-PHASE, TAPERED FLUIDIZED BED

MASSACHUSETTS INST. OF TECH., OAK RIDGE,
TENN. SCHOOL OF CHEMICAL ENGINEERING
PRACTICE

26 APR 1976

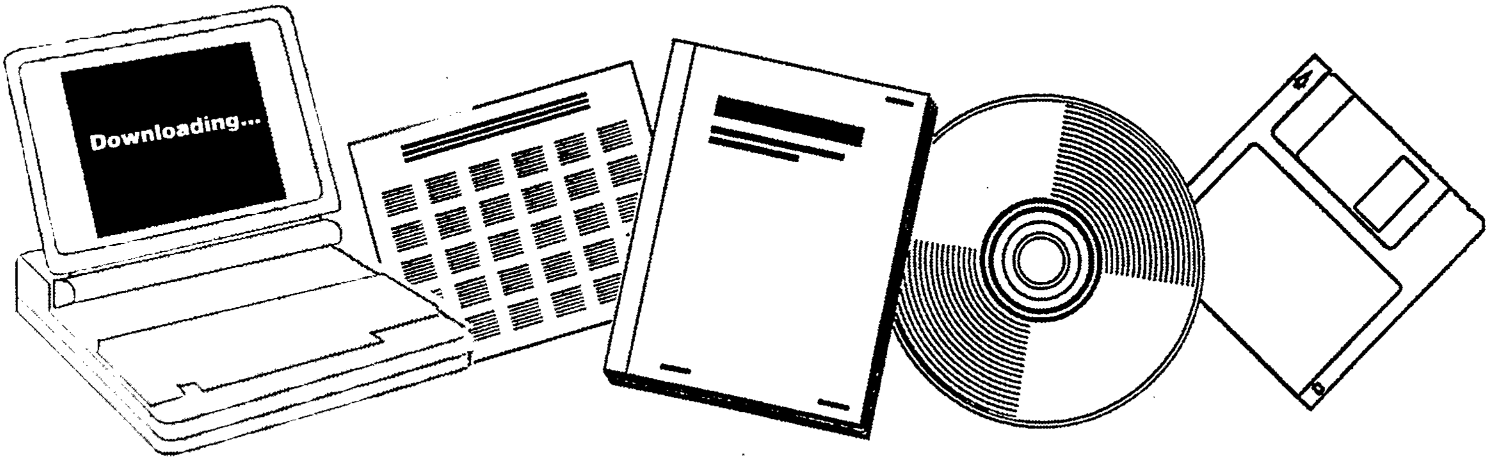
Downloading...

U.S. Department of Commerce
National Technical Information Service

One Source. One Search. One Solution.

NTIS

Providing Permanent, Easy Access to U.S. Government Information

National Technical Information Service is the nation's largest repository and disseminator of government-initiated scientific, technical, engineering, and related business information. The NTIS collection includes almost 3,000,000 information products in a variety of formats: electronic download, online access, CD-ROM, magnetic tape, diskette, multimedia, microfiche and paper.

Search the NTIS Database from 1990 forward

NTIS has upgraded its bibliographic database system and has made all entries since 1990 searchable on **www.ntis.gov.** You now have access to information on more than 600,000 government research information products from this web site.

Link to Full Text Documents at Government Web Sites

Because many Government agencies have their most recent reports available on their own web site, we have added links directly to these reports. When available, you will see a link on the right side of the bibliographic screen.

Download Publications (1997 - Present)

NTIS can now provides the full text of reports as downloadable PDF files. This means that when an agency stops maintaining a report on the web, NTIS will offer a downloadable version. There is a nominal fee for each download for most publications.

For more information visit our website:

www.ntis.gov

U.S. DEPARTMENT OF COMMERCE
Technology Administration
National Technical Information Service
Springfield, VA 22161

ORNLMIT231

OAK RIDGE NATIONAL LABORATORY
OPERATED BY
UNION CARBIDE CORPORATION
NUCLEAR DIVISION

POST OFFICE BOX X
OAK RIDGE, TENNESSEE 37830

ORNL/MIT- 231

DATE: April 26, 1976

COPY NO.

SUBJECT: Gas-Liquid Mass Transfer in a Three-Phase, Tapered Fluidized Bed

Authors: P.D. Terpandjian, J.P. D'Acierno, P. Stiros, and J.N. Vora

Consultants: C.W. Hancher and J.M. Begovich

ABSTRACT

The overall gas-liquid mass transfer coefficient, K_La, has been related to gas flow rate, solid particle size, and amount of solid charge for a cocurrent three-phase, tapered fluidized bed. The three phases consisted of oxygen, distilled water, and glass and coal particles from 0.15 to 0.56 mm OD. K_La was calculated on the basis of a well-mixed CSTR model. For a constant water flow rate of ∿750 ml/min and an oxygen flow rate between 600 to 1050 ml/min, the value of K_La appeared to be a maximum (∿1.8 min^{-1}) for a coal particle size of 0.3 mm. The value of K_La was not significantly affected by the amount of coal charged to the column. However, the value of K_La increased as the amount of glass in the bed decreased. Improvements to the experimental procedure and suggestions for future work are presented.

NOTICE

This report was prepared as an account of work sponsored by the United States Government. Neither the United States nor the United States Energy Research and Development Administration, nor any of their employees, nor any of their contractors, subcontractors, or their employees, makes any warranty, express or implied, or assumes any legal liability or responsibility for the accuracy, completeness or usefulness of any information, apparatus, product or process disclosed, or represents that its use would not infringe privately owned rights.

Oak Ridge Station
School of Chemical Engineering Practice
Massachusetts Institute of Technology

MASTER

BLANK PAGE

Printed in the United States of America. Available from
National Technical Information Service
U.S. Department of Commerce
5285 Port Royal Road, Springfield, Virginia 22161
Price: Printed Copy $4.00; Microfiche $2.25

This report was prepared as an account of work sponsored by the United States Government. Neither the United States nor the Energy Research and Development Administration/United States Nuclear Regulatory Commission, nor any of their employees, nor any of their contractors, subcontractors, or their employees, makes any warranty, express or implied, or assumes any legal liability or responsibility for the accuracy, completeness or usefulness of any information, apparatus, product or process disclosed, or represents that its use would not infringe privately owned rights.

Figures

		Page
1	Fluidized Bed Approximated by a Series of Stirred Tanks	7
2	Response Curve for Step Change in Feed Concentration	8
3	Experimental Apparatus	10
4	Experimental Response to Step Change in Feed Concentration	12
5	Effect of Bed Weight on $K_L a$	14
6	Effect of Solids Weight and Gas Flow Rate on $K_L a$	15
7	Effect of Solid Size on $K_L a$	16
8	Effect of Particle Size on $K_L a$	17

Contents

Page

1. Summary 4
2. Introduction 4
    2.1 Background 4
    2.2 Previous Work 4
    2.3 Mass Transfer Models 5
    2.4 Objectives and Method of Attack 9
3. Apparatus and Experimental Procedure 9
4. Results 11
5. Discussion of Results 11
6. Conclusions 18
7. Recommendations 18
8. Acknowledgments 19
9. Appendix 20
    9.1 Sample Calculations 20
    9.2 Derivation of Model Equations 20
    9.3 Location of Original Data 27
    9.4 Nomenclature 27
    9.5 Literature References 28

BLANK PAGE

1. SUMMARY

Experiments were performed to relate the gas-liquid mass transfer coefficient to gas flow rate, solid particle size, and amount of solid charged in a three-phase tapered fluidized bed. The tapered column was 42 in. high, 1-in. ID at the bottom, and 3-in. ID at the top. Coal and glass particles, oxygen, and distilled water were employed as the three phases. The mass transfer experiments were performed to measure the amount of oxygen that was transferred to the water phase. An oxygen analyzer probe measured the concentration of oxygen at the boundary between the two-phase and three-phase sections of the bed. For a known amount of solid charged to the column, the gas flow rate was set to four values in the range of 200-1100 ml/min. Four amounts of solid were charged to the column in the range from 200-1400 gm. Hence a total of sixteen oxygen concentration readings were recorded per size of solid. To study mixing within the column, dye tracer experiments were performed after each mass transfer experiment with the same operating conditions. The flow behavior was modeled as a series of continuously-stirred tank reactors (CSTR) and the K_La for each run determined.

K_La was plotted as a function of gas flow rate for a given size of coal and varying amounts of coal charged to the bed. The effect of coal size on K_La was also established. For glass particles only the effect of the amount charged to the bed on K_La was established. However, to choose between glass and coal to maximize the value of K_La will require additional data.

2. INTRODUCTION

2.1 Background

Three-phase fluidized bed reactors, consisting of solid particles fluidized by gas and liquid flows, have certain advantages over fixed beds as biochemical reactors (4). In tapered columns, biomass may accumulate without agglomeration or clogging. In addition, solid particles maintain a more stable bed height over a wider range of liquid and gas superficial velocities than in cylindrical columns due to the decrease of superficial and liquid and gas velocities with height. Experiments with tapered columns are required to measure gas-liquid mass transfer coefficient and establish operating conditions that will maximize mass transfer.

2.2 Previous Work

Saad _et al._ (1) have investigated the operating characteristics and mass transfer behavior in three-phase cylindrical fluidized beds with an air-CO_2 gas mixture, water, and 4x8 mesh alumina beads. They concluded that in the fluidized bed with 4x8 mesh alumina beads, the mass transfer behavior was best described by a plug flow model. Burck _et al._ (2)

indicated that the gas-liquid mass transfer coefficient for 4x8 mesh alumina beads in the same apparatus was best described by a plug flow model, whereas, for 0.25-in. plexiglas spheres, the flow behavior approached a CSTR model. They concluded that the gas-liquid mass transfer coefficient is affected by the density difference between the packing and the liquid.

The operation of three-phase fluidized beds has been reviewed by Østergaard (3), who discussed the role of gas-liquid mass transfer as the potential rate-limiting step in this type of reactor.

2.3 Mass Transfer Models

Mathematical models were developed for three different reactor flow models. The value of $K_L a$ can be calculated using these models under various sets of conditions, and hence a set of conditions can be found which gives maximum oxygen transferred from the gas phase to the liquid phase.

The value of the mass transfer coefficient calculated from known inlet and outlet concentrations and flow rates depends on the assumed column concentration profile which depends on the mixing in the column. Models for the plug flow and continuously stirred tank (CSTR) reactors were developed in which the liquid phase flow characteristics were assumed to be plug flow or well-mixed, respectively. The gas flow in both the models was assumed to be plug flow in nature. The theoretical concentration profiles were calculated from a steady state material balance around the column, Henry's Law, and an equation defining the mass transfer coefficient. The final equation relating the concentration and $K_L a$ for the CSTR model is,

$$K_L a = \frac{(AU_L C_L)_{out} - (AU_L C_L)_{in}}{(C_{L,eq} - C_{L,out})V} \qquad (1)$$

and for the plug flow model is,

$$K_L a = \frac{U_{L,in} r_{in}^2}{H^3}\left[\ln\left(\frac{B + 1}{B}\right)\right] \frac{3}{3\left(\frac{r_o}{H}\right)\left(\frac{r_o}{H} + \tan\theta\right) + \tan^2\theta} \qquad (2)$$

The differential equation for the liquid plug flow with axial dispersion is,

$$\varepsilon D(r_o + h\tan\theta)^2 \frac{d^2C_L}{dh^2} - [U_{Lo} r_o^2 - 2\varepsilon D(r_o + h\tan\theta)\tan\theta] \frac{dC_L}{dh}$$
$$= -K_L a(C_{L,eq} - C_L)(r_o + h\tan\theta)^2 \qquad (3)$$

Equations (1) and (2) are derived in Appendix 10.2. Equation (3) was not evaluated because the value of dispersion coefficient, D, or the variation of C with column height were not known.

Without solving the differential equation, the bed can be simulated by n ideal stirred tanks in series as shown in Fig. 1. The total volume of the tanks, V_t, is the same as the volume of the three-phase fluidized bed. Thus, for a given flow rate, the total mean residence time, $\bar{t}$, is also the same. The mean residence time per tank is $\bar{t}/n$ and the volume of each tank is V_t/n.

The value of n can be found by tracer dispersion experiments. If a step input of a tracer is introduced at the inlet of n tanks, the concentration - neglecting mass transfer between phases - as a function of time can be calculated for various values of n with Eq. (4).

$$\left(\frac{C_n}{C_0}\right)_{step} = 1 - e^{-nt/\bar{t}}\left[1 + \frac{nt}{\bar{t}} + \frac{1}{2!}\left(\frac{nt}{\bar{t}}\right)^2 + \ldots\right.$$
$$\left. + \frac{1}{(n-1)!}\left(\frac{nt}{\bar{t}}\right)^{n-1}\right] \qquad (4)$$

Thus, the theoretical values of C_n/C_0 as a function of $t/\bar{t}$ for various values of n is as shown in Fig. 2. Experimentally measured values of C_n/C_0 can be plotted against $t/\bar{t}$ and superimposed on this figure. By comparison the value of n can be determined, and the volume of each stirred tank can be calculated.

If the concentration of oxygen is measured in the inlet stream, concentration of oxygen in the stream leaving the first stage can be calculated with Eq. (1) for a trial value of K_La. The oxygen concentration in the liquid stream entering the second tank is the same as the stream leaving the first tank. Assuming K_La is constant in all the tanks, the oxygen concentration in the liquid stream leaving the second tank can also be calculated with Eq. (1). Thus, if a value for K_La is assumed and if it is assumed that the concentration of oxygen in the liquid stream entering any tank is the same as in the liquid stream leaving the previous tank, the oxygen concentration can be calculated for the series of stirred tanks. The concentration in the stream leaving the bed, which is the same as in the stream leaving the nth tank, can be calculated. The assumed value of K_La can be checked by comparing the calculated value of oxygen in the liquid stream leaving the bed with the value measured experimentally. Thus the value of K_La can be determined by a trial and error calculation.

This method can be used for plug flow, CSTR, or plug flow with axial dispersion models. For mixing similar to a CSTR or plug flow reactor, the value of n will be one or infinity, respectively; while a plug flow reactor with axial dispersion behavior corresponds to a value of n between one and

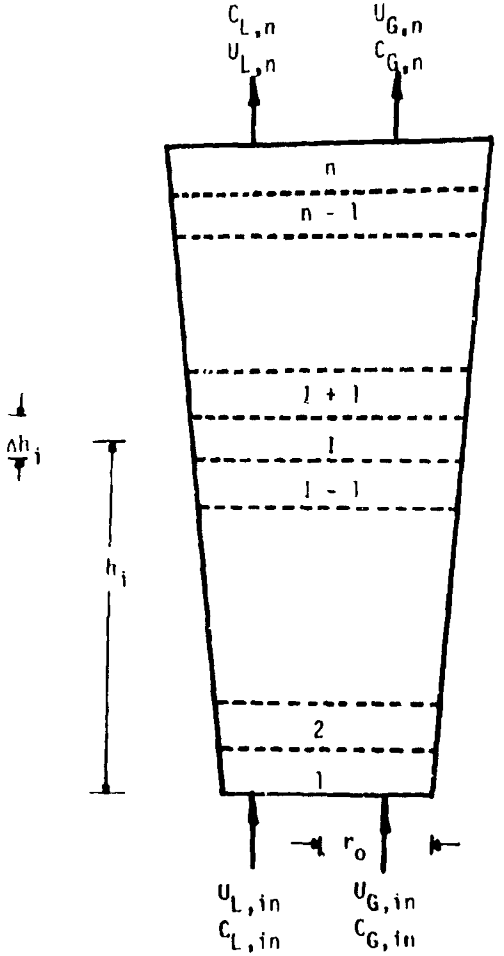
$C_{L,n}$
$U_{L,n}$
$U_{G,n}$
$C_{G,n}$
n
n - 1
i + 1
i
i - 1
2
1
Δh_i
h_i
r_0
$U_{L,in}$
$C_{L,in}$
$U_{G,in}$
$C_{G,in}$

$$\Delta V_1 = \Delta V_2 = \ldots\ldots = \Delta V_n$$

$$\Delta V_i = \pi(r_0 + h_i \tan\theta)^2 \, \Delta h_i + \pi(r_0 + h_i \tan\theta)\tan\theta \, \Delta h_i^2 + \frac{\pi}{3}\tan^2\theta \, \Delta h_i^3$$

MASSACHUSETTS INSTITUTE OF TECHNOLOGY
SCHOOL OF CHEMICAL ENGINEERING PRACTICE
AT
OAK RIDGE NATIONAL LABORATORY

FLUIDIZED BED APPROXIMATED
BY A SERIES OF STIRRED TANKS

DATE	DRAWN BY	FILE NO.	FIG.
4-24-76	JHV	CEPS-X-231	1

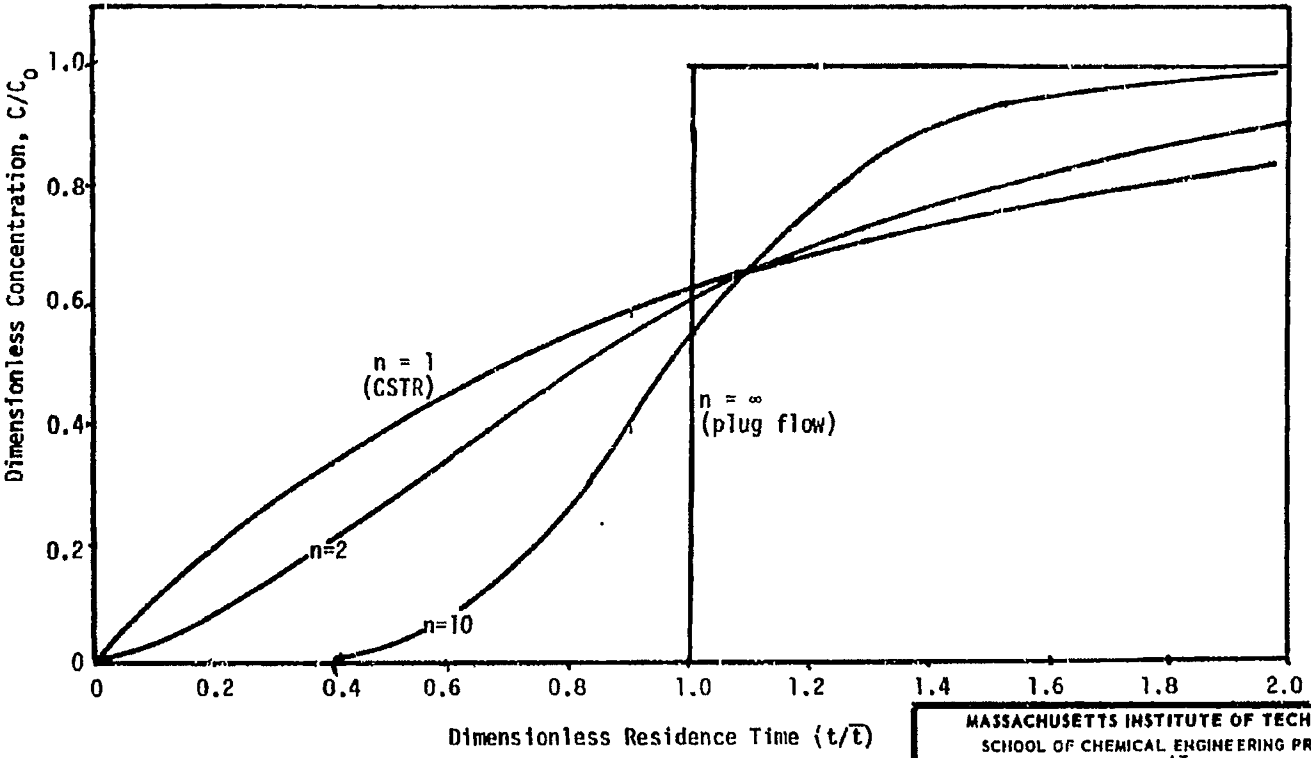

MASSACHUSETTS INSTITUTE OF TECHNOLOGY
SCHOOL OF CHEMICAL ENGINEERING PRACTICE
AT
OAK RIDGE NATIONAL LABORATORY

RESPONSE CURVE FOR STEP CHANGE
IN FEED CONCENTRATION

DATE	DRAWN BY	FILE NO.	FIG.
4-24-76	JNV	CEPS-X-231	2

infinity. As the axial dispersion becomes large, the value of n will approach one. In the extreme case, when the axial dispersion is so large that the concentration throughout the bed is uniform, the value of n will be one and the bed will have the characteristics of a CSTR.

2.4 Objectives and Method of Attack

The objectives were to relate K_La to the size and total weight of fluidized solid and to gas flow rate. Then, it should be possible to select a combination of these parameter values to maximize K_La.

Analytical equations that describe the transfer of oxygen from the gas phase to the liquid phase were derived for three liquid flow models in a cocurrent column. Tracer experiments were then performed to characterize the dispersion flow behavior in the column. Models of fluid flow for CSTR behavior and for a plug flow reactor with and without axial dispersion were derived for the tapered bed. To determine which behavior was applicable, the transient concentration of a dye at the level between the three and two-phase regions of the bed was measured for a step input of dye. From this residence time distribution, the flow behavior was established. Finally, experiments were performed to measure and correlate the mass transfer coefficient at various operating conditions. The dissolved oxygen concentration in the bed was measured with four different amounts of coal and glass fluidized in the bed in four particle sizes. The available sizes ranged in diameter from 0.15 to 0.3 mm. The mass transfer parameter, K_La, was then determined from the CSTR model and plotted as a function of gas flow rate.

3. APPARATUS AND EXPERIMENTAL PROCEDURE

The gas-liquid mass transfer coefficient for oxygen was determined in the tapered pyrex column shown in Fig. 3. Glass or coal particles in the column were fluidized by the cocurrent upward flow of oxygen and water. Experimental conditions included four values of gas flow rate between 200 and 1100 ml/min and four amounts of solids in the bed for a liquid flow rate of about 760 ml/min.

Before the desired amount of solids was placed in the column, the water flow rate was adjusted with a metering pump and measured at the liquid discharge. Inlet distilled water was stripped of residual oxygen with a stream of nitrogen passed countercurrently through a cylindrical glass column. Oxygen dissolved in water was measured with an IL 530 oxygen electrode. With this apparatus a 12-in. probe, 0.75-in.-OD, measures the conductance of the liquid stream which is proportional to the concentration of dissolved oxygen in water. The output is indicated on a recorder as ppm of oxygen.

The oxygen flow rate to the tapered column was adjusted with a needle valve on the inlet line and measured at the top of the column with a wet

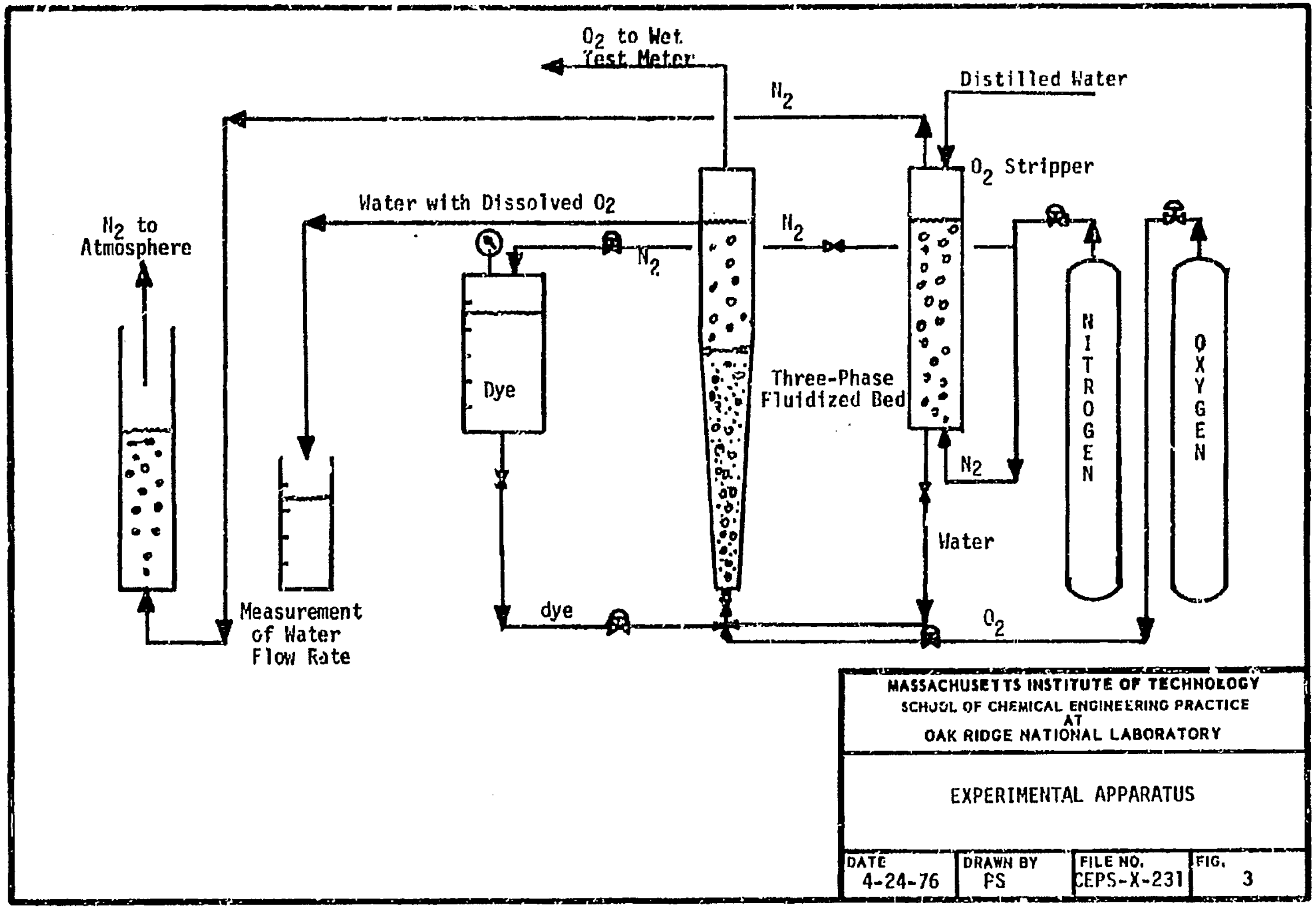
O_2 to Wet Test Meter
N_2
Distilled Water
O_2 Stripper
Water with Dissolved O_2
N_2 to Atmosphere
N_2
N_2
Dye
Three-Phase Fluidized Bed
NITROGEN
OXYGEN
N_2
Water
Measurement of Water Flow Rate
dye
O_2

MASSACHUSETTS INSTITUTE OF TECHNOLOGY
SCHOOL OF CHEMICAL ENGINEERING PRACTICE
AT
OAK RIDGE NATIONAL LABORATORY

EXPERIMENTAL APPARATUS

DATE	DRAWN BY	FILE NO.	FIG.
4-24-76	PS	CEPS-X-231	3

test meter. The oxygen analyzer probe was placed near the top of the column to measure the dissolved oxygen with minimum effect on fluid flow in the three-phase bed. Steady state mass transfer in the fluidized bed was determined from the transient plot of oxygen concentration on a strip chart recorder. When steady state had been achieved, the oxygen probe was lowered to measure the dissolved oxygen concentration at the boundary between the three and two-phase regions.

An experiment was performed to determine the number of hypothetical uniformly-stirred tanks of equal volume which could best approximate the mixing and flow characteristics of the three-phase bed. An aqueous solution of rhodamine B dye was mixed in a 3/8-in.-diam tee with water flowing into the column. A constant pressure of 6 psig was maintained in the dye storage tank with nitrogen. A needle valve, adjusted for the desired flow rate, was installed in series with a ball valve to maintain a constant and instantaneous flow rate of concentrated dye solution into the tee. The maximum flow rate of dye was 3% of total water flow. Ten milliliter samples of the liquid were removed at a level in the bed between the two and three-phase regions using a 3/8-in.-diam tube with a porous disk mounted on the end to prevent solids from entering with the samples. The time was recorded when each sample was removed. When the color of the samples did not change, a dye solution sample was taken from the tee located on the inlet line to the column. The concentration of the dye in each sample was measured with an optical spectrophotometer and with distilled water as a blank.

4. RESULTS

The transient response to a step change in concentration of a dye solution was established as shown in Fig. 4. The effect of bed weight on K_La is shown in Fig. 5 for glass particles and in Fig. 6 for coal particles. In both figures K_La is plotted as a function of gas flow rate for various bed weights.

The effect of coal particle size on K_La is shown in Fig. 7 using average values for total solids weight from Fig. 6. In Fig. 8 the effect of gas flow rate on K_La is established.

5. DISCUSSION OF RESULTS

The transient dimensionless concentration for a step change in the inlet concentration of rhodamine B dye solution into the tapered bed, with fluidized 0.30 mm coal particles, is shown as a function of dimensionless time in Fig. 4. The experimental curve is superimposed on the theoretical curves which depict residence time distribution for plug flow as well as for one, two, and an infinite number of well-mixed tanks in series. Similar trends were shown for 0.15, 0.45, and 0.57-mm coal particles. Because

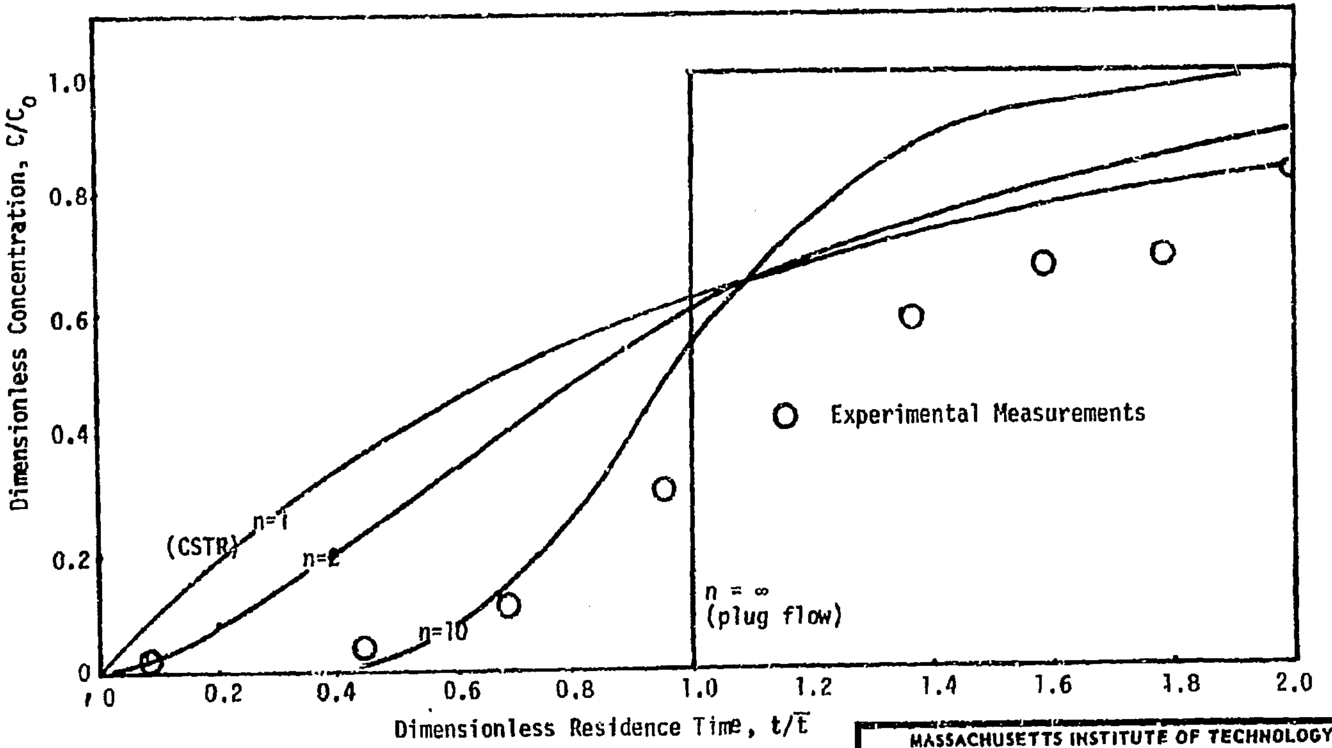

MASSACHUSETTS INSTITUTE OF TECHNOLOGY
SCHOOL OF CHEMICAL ENGINEERING PRACTICE
AT
OAK RIDGE NATIONAL LABORATORY

EXPERIMENTAL RESPONSE TO STEP CHANGE IN FEED CONCENTRATION

DATE	DRAWN BY	FILE NO.	FIG.
4-24-76	JNV	CEPS-X-231	4

transient behavior follows an exponential pattern and the results for all experiments showed that the concentration does not equal the inlet value until ten residence times elapse, it is concluded that plug flow behavior does not occur in the tapered bed. It was assumed that the tapered fluidized bed behaves as one CSTR in order to compare all results for oxygen transfer.

The overall mass transfer coefficient, K_La, was calculated for various amounts of 0.17-0.18-mm glass particles fluidized in the tapered bed, and the values were correlated in Fig. 5 as a function of gas flow rate for a constant water flow rate of approximately 760 ml/min. The results show a unique trend for each amount of glass fluidized in the bed. All trends show that the amount of oxygen transferred into the liquid phase increases linearly with gas flow rate. The mass transfer coefficient, K_La, decreases as the amount of solids in the bed is increased. Because the size of the gas bubbles leaving the bed increased as more solids were added to the bed, the decrease in the interfacial surface area, a, between oxygen and water per unit bed volume may be the cause of this trend.

Figure 6 is an analogous representation of mass transfer for various amounts of 0.3-mm coal particles in the bed as a function of gas flow rate. The general trend, which was the same for coal particles of sizes 0.15 and 0.56 mm, is an increase in the mass transfer coefficient, K_La, with an increase in gas flow rate through the bed. As shown in Fig. 6, the crowded data for 150 to 300 gm of coal in the bed shows that the solid weight of the bed does not substantially change the oxygen transfer. For this reason, the data for each size particle with varying amounts of solids was averaged at the four gas flow rates and are shown in Fig. 7.

Figure 7 shows the effect of gas flow rate on the overall mass transfer coefficient for three sizes of coal as well as for the bed without solids present. Each point on this graph represents the averaged results of four experiments. This figure shows that the use of 0.30-mm coal particles in the bed will give the best transfer of oxygen, and this system will operate more effectively than with two-phase transfer. The largest size of coal, 0.56 mm, gives the smallest rate of oxygen transfer while the smallest size, 0.30 mm, exhibits behavior which is nearest to that for a two-phase system. These results show that the highest values of K_La will occur for operation with 0.30-mm coal particles at gas flow rates greater than 400 ml/min.

Figure 8 shows the same data points plotted as a function of coal particle size for the four gas flow rates. The oxygen transfer dependence on coal particle size is shown to increase as the gas flow rate is increased. The strongest dependence of K_La on flow rate is for the medium sized particle.

The results for coal and glass cannot be compared to determine which type of solid will provide the best mass transfer of oxygen in the column. However, if large surface area per weight of packing in the column is necessary, coal will probably be better than glass since K_La decreases as more glass is added to the fluidized bed, while K_La for coal does not exhibit as strong a dependence. The optimum transfer of oxygen in the bed

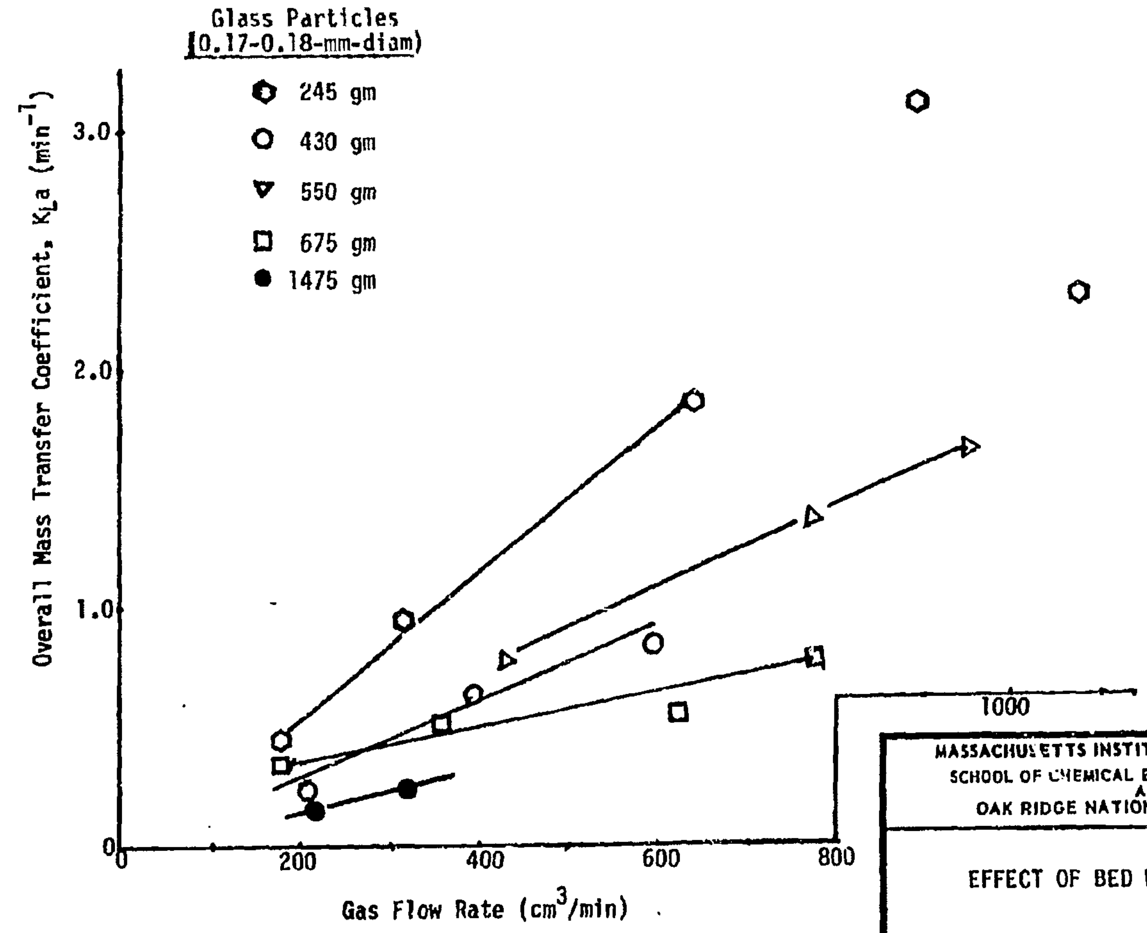

MASSACHUSETTS INSTITUTE OF TECHNOLOGY
SCHOOL OF CHEMICAL ENGINEERING PRACTICE
AT
OAK RIDGE NATIONAL LABORATORY

EFFECT OF BED WEIGHT ON K_La

DATE	DRAWN BY	FILE NO.	FIG.
4-24-76	JNV	CEPS-X-231	5

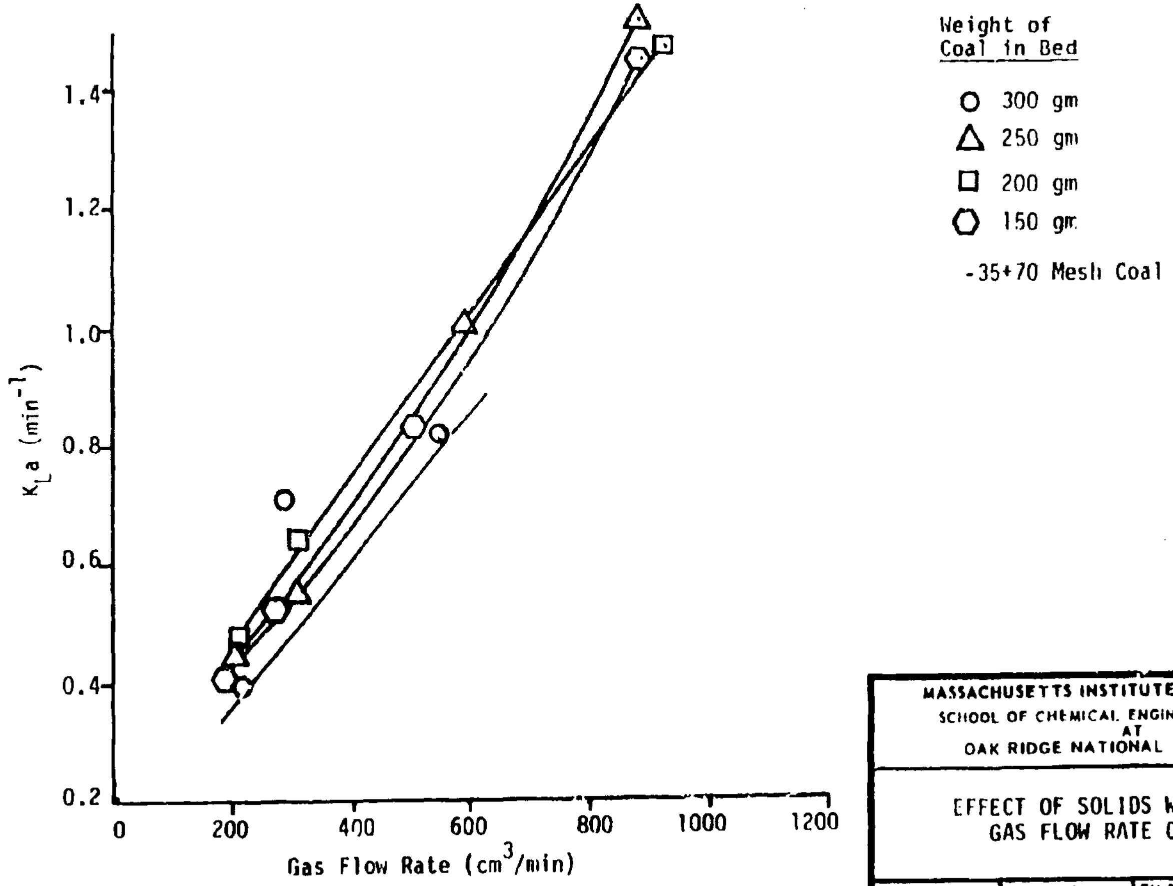

MASSACHUSETTS INSTITUTE OF TECHNOLOGY
SCHOOL OF CHEMICAL ENGINEERING PRACTICE
AT
OAK RIDGE NATIONAL LABORATORY

EFFECT OF SOLIDS WEIGHT AND
GAS FLOW RATE ON K_La

DATE	DRAWN BY	FILE NO.	FIG.
4-24-76	JNV	CEPS-X-231	6

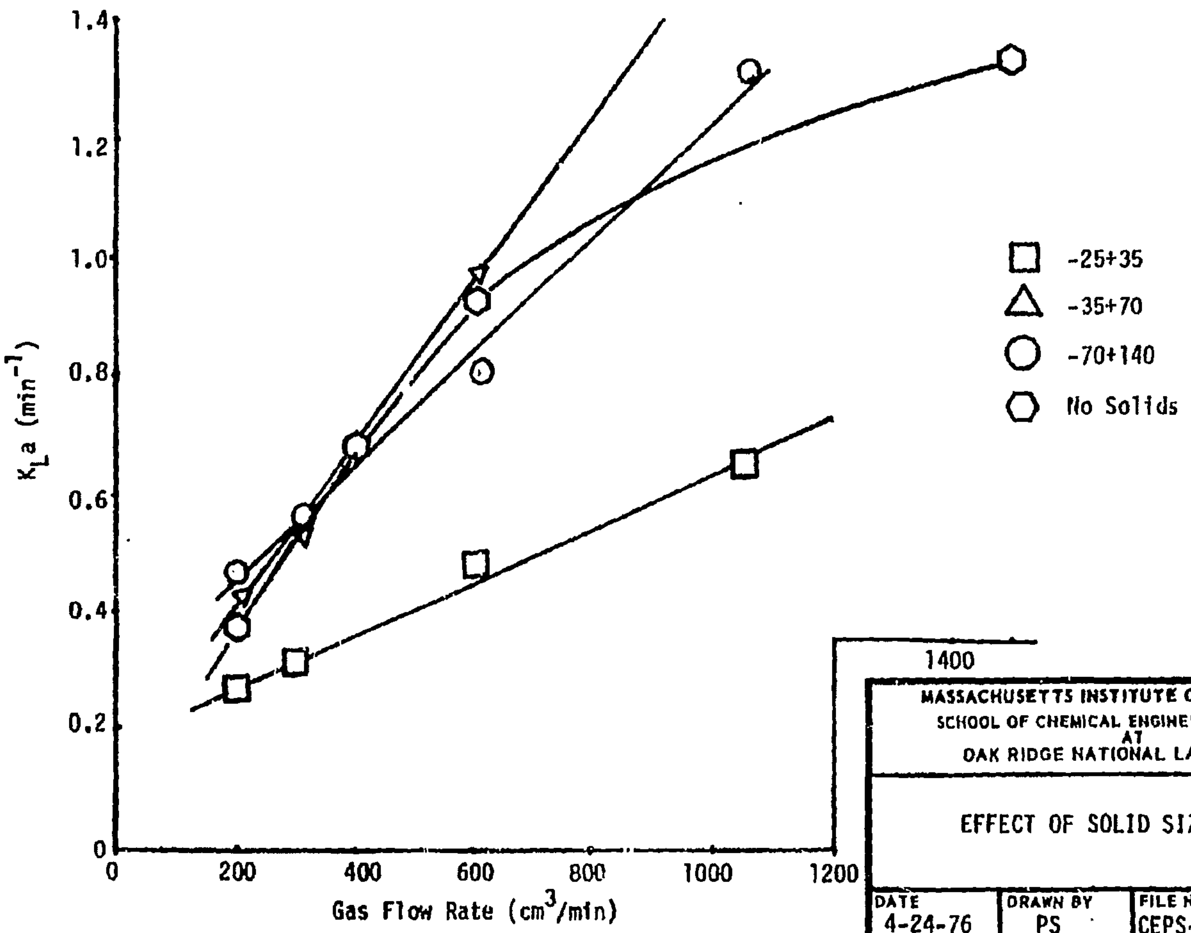

MASSACHUSETTS INSTITUTE OF TECHNOLOGY
SCHOOL OF CHEMICAL ENGINEERING PRACTICE
AT
OAK RIDGE NATIONAL LABORAT RY

EFFECT OF SOLID SIZE ON $K_L a$

DATE	DRAWN BY	FILE NO.	FIG.
4-24-76	PS	CEPS-X-231	7

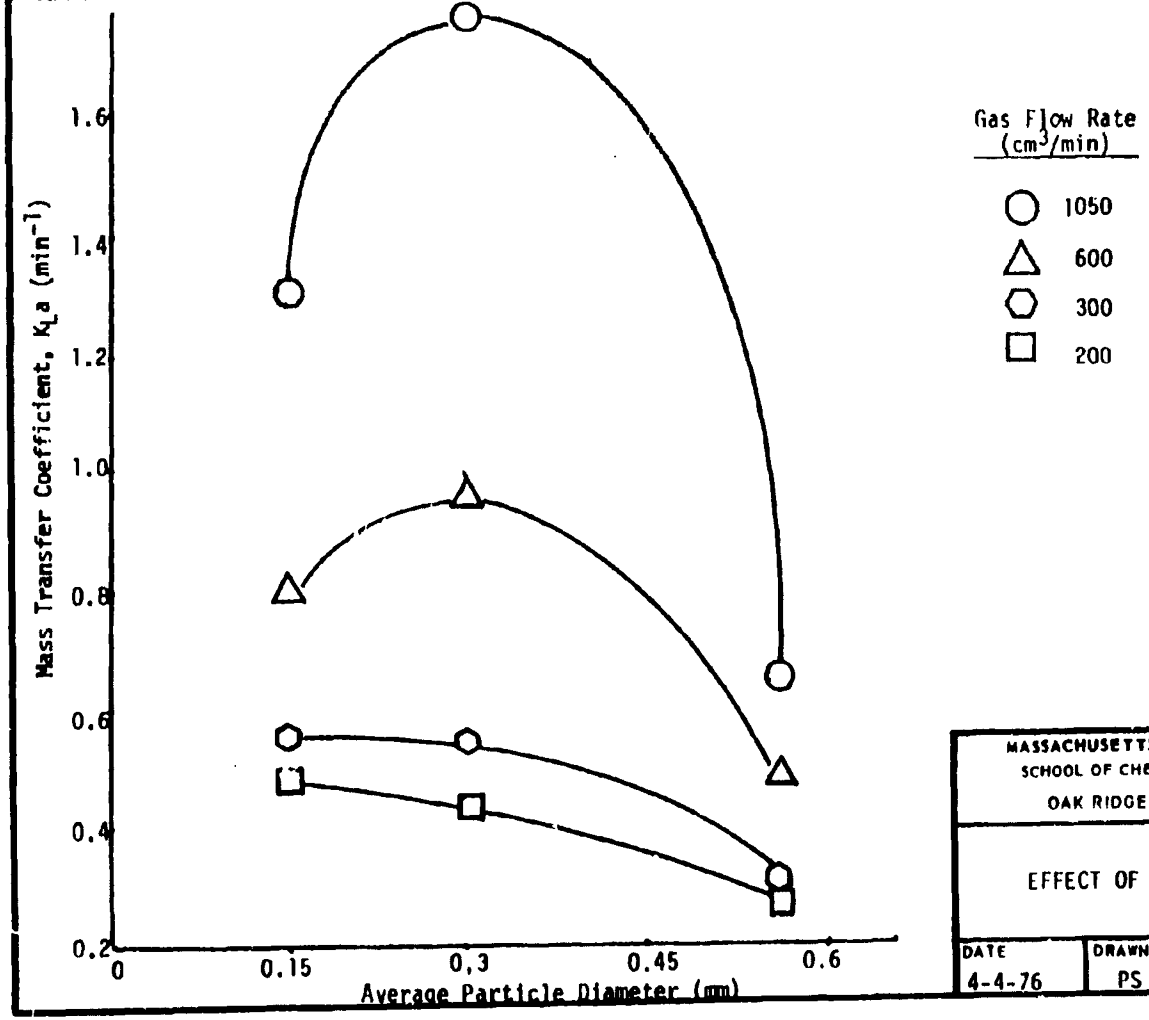

MASSACHUSETTS INSTITUTE OF TECHNOLOGY
SCHOOL OF CHEMICAL ENGINEERING PRACTICE
AT
OAK RIDGE NATIONAL LABORATORY

EFFECT OF PARTICLE SIZE ON K_La

DATE	DRAWN BY	FILE NO.	FIG.
4-4-76	PS	CEPS-X-231	8

for fluidized coal in the experimental tapered bed will occur with 0.30-mm size particles at gas flow rates greater than 400 ml/min.

Values of K_La for the tapered bed operating without fluidized solids are shown in Table 1. Oxygen transfer decreases as liquid flow rate decreases for a given gas flow rate. From these limited results, it is recommended that the effect of liquid flow rate on K_La should also be investigated for optimization of mass transfer in the bed.

Table 1. Mass Transfer for Two-Phase System

Flow Rates (ml/min)		K_La
Water	Oxygen	(min^{-1})
735	250	0.253
890	250	0.238
1062	250	0.232
1176	250	0.200

6. CONCLUSIONS

At constant liquid flow rate (∿750 ml/min),

- K_La increases as gas flow rate increases for both glass and coal particles.
- For coal particles only,
  - The value for K_La is maximized with the 0.3-mm particle size for gas flow rates between 600 and 1050 cm^3/min.
  - K_La decreases as particle size increases for gas flow rates less than 300 cm^3/min.
- The amount of coal particles does not significantly affect K_La. However, for the glass particles, the value of K_La increases as the amount of glass in the bed decreases.

7. RECOMMENDATIONS

1. Determine oxygen concentration as a function of bed height.

2. Calculate K_La with a numerical integration of the curve obtained by plotting $(C_{L,eq} - C_L)$ as a function of bed volume:

$$K_La = \frac{Q_w(C_{L,out} - C_{L,in})}{\int_0^V (C_{L,eq} - C_L)dV}$$

3. Perform more experiments to correlate K_La with particle density.

4. Determine effect of varying liquid flow rate on K_La.

8. ACKNOWLEDGMENTS

The authors would like to thank their consultants, C.W. Hancher and J.M. Begovich, for their help during the project.

9. APPENDIX

9.1 Sample Calculations

9.1.1 Tapered Reactor Volume

The total volume of the tapered reactor of base radius, r_1, top radius, r_2, and height, h, is given by

$$V = \frac{\pi h}{3}[r_1^2 + r_1 r_2 + r_2^2]$$

For Run 1,

$$r_1 = 1.27 \text{ cm}$$

$$h = 61.5 \text{ cm}$$

$$r_2 = r_1 + h \tan \theta = 1.27 + 61.5 \tan(1.33) = 2.67 \text{ cm}$$

Thus,

$$V = \frac{\pi(61.5)}{3}[(1.27)^2 + (1.27)(2.67) + (2.67)^2] = 792 \text{ cm}^3$$

9.1.2 K_La

For each run, the overall mass transfer coefficient, K_La, was calculated by approximating the reactor liquid flow behavior as a single well-mixed tank. Thus, K_La is given by the equation,

$$K_La = \frac{Q_w(C_{L,out} - C_{L,in})}{V(C_{L,eq} - C_{L,out})} = \frac{50.6 \text{ cm}^3/\text{min}(20 - 0 \text{ ppm})}{792 \text{ cm}^3(39 - 20 \text{ ppm})}$$

$$= 0.673 \text{ min}^{-1}$$

9.2 Derivation of Model Equations

The assumptions made when performing material balances on the tapered bed are: K_La is independent of height in the column, the solute concentration is so dilute that a linear equilibrium relationship applies, the dispersion coefficient and void fraction in the column are constant, and the liquid density is constant.

In a continuously stirred tank reactor, CSTR, the concentration in the reactor is assumed to be the same as the concentration in the exit stream. At steady state, an oxygen mass balance gives

$$\text{input} - \text{output} = 0 \qquad (5)$$

The oxygen input and output for the reactor includes oxygen in the gas phase and dissolved oxygen in the water.

$$[\dot{M} + AU_L C_L]_{in} - [\dot{M} + AU_L C_L]_{out} = 0 \qquad (6)$$

If $K_L a$ is constant throughout the reactor, then the rate of oxygen mass transfer from the gas phase to the liquid phase in the bed is

$$N_{O_2} = K_L aV(C_{L,eq} - C_L) \qquad (7)$$

Thus,

$$K_L a = \frac{AU_L C_L|_{out} - AU_L C_L|_{in}}{(C_{L,eq} - C_L)V} \qquad (8)$$

9.2.1 Model II, Dispersion Model Calculation of $K_L a$

To calculate $K_L a$, an oxygen balance on a differential element of the reactor shown in Fig. 1 must be performed.

$$\text{input} - \text{output} = 0$$

$$\begin{bmatrix} \text{gas} & & \text{liquid phase} & & \text{liquid phase} \\ \text{phase} & + & \text{input by} & + & \text{input by} \\ \text{input} & & \text{convection} & & \text{dispersion} \end{bmatrix} - \begin{bmatrix} \text{gas} & & \text{liquid phase} & & \text{liquid phase} \\ \text{phase} & + & \text{output by} & + & \text{output by} \\ \text{output} & & \text{convection} & & \text{dispersion} \end{bmatrix} = 0 \qquad (9)$$

$$[AU_GC_G + AU_LC_L - A\varepsilon D\,\frac{dC_L}{dh}]_{\text{at element inlet } h}$$

$$- [AU_GC_G + AU_LC_L - A\varepsilon D\,\frac{dC_L}{dh}]_{\text{at element outlet } h+\Delta h} = 0 \quad (10)$$

or taking the limit as Δh approaches zero gives

$$\frac{d(AU_GC_G)}{dh} + \frac{d(AU_LC_L)}{dh} - \frac{d}{dh}(A\varepsilon D\,\frac{dC_L}{dh}) = 0 \quad (11)$$

If ε and D are constant, expansion of the second and third differentials gives,

$$\frac{d}{dh}(AU_LC_L) = [(U_LC_L)\,\frac{dA}{dh} + (U_LA)\,\frac{dC_L}{dh} + (AC_L)\,\frac{dU_L}{dh}$$

and

$$\frac{d}{dh}(A\varepsilon D\,\frac{dC_L}{dh}) = \varepsilon D[(\frac{dA}{dh})(\frac{dC_L}{dh}) + A\,\frac{d^2C_L}{dh^2}]$$

If one substitutes the relations

$$\frac{dA}{dh} = 2\pi(r_o + h\tan\theta)\tan\theta$$

and

$$\frac{dU_L}{dh} = -\frac{2U_{Lo}r_o^2\tan\theta}{(r_o + h\tan\theta)^3}$$

into the differential equation, one obtains

$$-\frac{d(AU_GC_G)}{dh} = \Big[(U_LC_L)2\pi(r_o + h\tan\theta)\tan\theta + U_LA\frac{dC_L}{dh} + (AC_L)[-\frac{2U_{L_o}r_o^2\tan\theta}{(r_o + h\tan\theta)^3}]\Big] - \varepsilon D[2\pi(r_o+h\tan\theta)\tan\theta\frac{dC_L}{dh} + A\frac{d^2C_L}{dh^2}]$$

Further substitution of

$$A = \pi(r_o + h\tan\theta)^2$$

and

$$U_L = \frac{U_{L_o}A_o}{A_1} = \frac{U_{L_o}r_o^2}{(r_o + h\tan\theta)^2}$$

into the equation gives

$$-\frac{d}{dh}(AU_GC_G) = [U_{L_o}r_o^2\pi - 2\pi\varepsilon D(r_o + h\tan\theta)\tan\theta]\frac{dC_L}{dh} - \pi\varepsilon D(r_o + h\tan\theta)^2\frac{d^2C_L}{dh^2} \qquad (12)$$

The amount of oxygen transferred from the gas phase to the liquid phase in the finite element, dh, of Fig. 1 is

$$-\Delta(AU_GC_G = K_La(C_{L,eq} - C_L)\Delta V$$

Since

$$\Delta V_i = \pi(r_o + h_i\tan\theta)^2\Delta h_i + \pi(r_o + h_i\tan\theta)\tan\theta(\Delta h_i)^2 + \frac{\pi\tan^2\theta}{3}(\Delta h_i)^3$$

$$dV = \pi(r_o + h\tan\theta)^2 dh$$

and

$$-\frac{d(AU_G C_G)}{dh} = K_L a(C_{L,eq} - C_L)\pi(r_o + h\tan\theta)^2 \qquad (13)$$

Hence,

$$-\pi\varepsilon D(r_o + h\tan\theta)^2 \frac{d^2C_L}{dh^2} + [U_{L_o} r_o^2 \pi - 2\pi\varepsilon D(r_o + h\tan\theta)\tan\theta]\frac{dC_L}{dh}$$

$$= K_L a(C_{L,eq} - C_L)\pi(r_o + h\tan\theta)^2$$

After rearrangement, the differential equation for plug flow with dispersion for the tapered column becomes

$$\varepsilon D(r_o + h\tan\theta)^2 \frac{d^2C_L}{dh^2} - [U_{L_o} r_o^2 - 2\varepsilon D(r_o + h\tan\theta)\tan\theta]\frac{dC_L}{dL}$$

$$= -K_L a(C_{L,eq} - C_L)(r_o + h\tan\theta)^2 \qquad (14)$$

If the equation is made dimensionless by substituting

$$Z = \frac{h}{H}$$

and

$$X = \frac{C_{L,out} - C_L}{C_{L,out} - C_{L,in}}$$

the differential equation takes the form,

$$\varepsilon D\left(\frac{r_o}{H} + Z\tan\theta\right)^2 \frac{d^2X}{dZ^2} - \left[\frac{U_{L_o} r_o^2}{H} - 2\varepsilon D\left(\frac{r_o}{H} + Z\tan\theta\right)\tan\theta\right]\frac{dX}{dZ}$$

$$= K_L a\left[\frac{C_{L,eq} - C_{L,out}}{C_{L,out} - C_{L,in}} + X\right]H^2\left(\frac{r_o}{H} + Z\tan\theta\right)^2 \qquad (15)$$

This non-linear second order differential equation was solved only for the limiting case of no dispersion; i.e., $D = 0$. Thus the equation becomes

$$-\frac{U_{L_o} r_o^2}{H}\frac{dX}{dZ} = K_L a H^2 \left(\frac{r_o}{H} + Z\tan\theta\right)^2 \left(\frac{C_{L,eq} - C_{L,out}}{C_{L,out} - C_{L,in}} + X\right)$$

If one defines

$$B = \frac{C_{L,eq} - C_{L,out}}{C_{L,out} - C_{L,in}}$$

and rearranges the equation, one obtains the differential equation

$$-\frac{U_{L_o} r_o^2}{H^3 K_L a}\frac{dX}{(B+X)} = -\left(\frac{r_o}{H} + Z\tan\theta\right)^2 dZ$$

with the boundary conditions

$$X = 1 \quad \text{at } Z = 0 \tag{16}$$

$$X = 0 \quad \text{at } Z = 1 \tag{17}$$

the above equation may be integrated to obtain

$$-\int_0^1 \frac{U_{L_o} r_o^2}{K_L a H^3}\frac{dX}{(B+X)} = \int_1^0 \left(\frac{r_o}{H} + Z\tan\theta\right)^2 dZ$$

or

$$\frac{U_{L_o} r_o^2}{K_L a H^3}\left[\ln\left(\frac{B+1}{B}\right)\right] = \left(\frac{r_o}{H}\right)^2 + \frac{r_o}{H}\tan\theta + \frac{\tan^2\theta}{3}$$

Hence,

$$K_L a = \frac{U_{L_o} r_o^2}{H^3}\left[\ln\left(\frac{B+1}{B}\right)\right]\frac{3}{3\left(\frac{r_o}{H}\right)\left(\frac{r_o}{H} + \tan\theta\right) + \tan^2\theta} \tag{18}$$

where:

$$B = \frac{C_{L,eq} - C_{L,out}}{C_{L,out} - C_{L,in}}$$

9.2.2 Volume of an Increment of Reactor Volume

The volume of an increment in the tapered column at a height, h_i, from the bottom and thickness Δh_i can be calculated by the equation as shown in Fig. 1.

ΔV_i = volume of the ith element

$$\Delta V = \frac{\pi \Delta h}{3}[r_1^2 + r_1 r_2 + r_1^2] \tag{19}$$

r_1 and r_2 can be written in terms of r_o, h_i, and θ:

$$r_1 = r_o + h_i \tan\theta \tag{20}$$

$$r_2 = r_o + h_i \tan\theta + \Delta h_i \tan\theta \tag{21}$$

Substituting this in the above equation gives

$$\begin{aligned}
\Delta V &= \frac{\pi \Delta h_i}{3}\Big[(r_o + h_i \tan\theta)^2 + (r_o + h_i \tan\theta)(r_o + h_i \tan\theta + \Delta h_i \tan\theta) \\
&\qquad + (r_o + h_i \tan\theta + \Delta h_i \tan\theta)^2\Big] \\
&= \frac{\pi \Delta h_i}{3}\Big[(r_o + h_i \tan\theta)^2 + (r_o + h_i \tan\theta)^2 + (r_o + h_i \tan\theta)\tan\theta \Delta h_i \\
&\qquad + (r_o + h_i \tan\theta)^2 + 2(r_o + h_i \tan\theta)\Delta h_i \tan\theta + \Delta h_i^2 \tan^2\theta\Big] \\
&= \frac{\pi \Delta h_i}{3}[3(r_o + h_i \tan\theta)^2 + 3(V_o + h_i \tan\theta)\tan\theta\ \Delta h_i + \Delta h_i^2 \tan^2\theta] \\
&= \pi(r_o + h_i \tan\theta)^2 \Delta h_i + \pi(r_o + h_i \tan\theta)\tan\theta(\Delta h)^2 + \frac{\pi \tan^2\theta}{3}(\Delta h)^3
\end{aligned} \tag{22}$$

9.3 Location of Original Data

The original data are located in ORNL Databook A-7023-G, pp. 43-84, on file at the MIT School of Chemical Engineering Practice, Bldg. 3001, ORNL.

9.4 Nomenclature

a	gas-liquid interfacial surface area per unit volume, cm^2/cm^3
A	column cross-sectional area, cm^2
B	dimensionless concentration, $\frac{C_{L,eq} - C_{L,out}}{C_{L,out} - C_{L,in}}$, (gm/cm^3)/(gm/cm^3)
C	concentration, gm/cm^3 (liquid)
D	eddy diffusivity, cm^2/sec
h	height, cm
H	total height of the bed, cm
K_L	overall gas-liquid mass transfer coefficient, gm/cm^2-sec(gm/cm^3)
$\dot{M}$	oxygen mass flow rate, gm/sec
N_{O_2}	amount of oxygen transfer per unit time in the bed, lb/cm^3-sec
Q_W	volumetric liquid flow rate, cm^3/min
r	radius, cm
U	superficial velocity, cm/sec
t	time, sec
$\overline{t}$	residence time, sec
X	dimensionless concentration
V	volume of reactor, cm^3
Z	dimensionless height, h/H,

Subscripts

0,1,2	position at height 0, h_1, and h_2
i, n	related to ith or nth stirred tank, respectively
G	gas phase
in	at inlet
L	liquid phase
L,eq	liquid phase at equilibrium
out	at outlet

Greek Symbols

ε	void fraction
Δ	finite increment
θ	tapered angle

9.5 References

1. Saad, E.T., H.D. Ayala, W.M. Burke, and D.K. Clarkson, "Cocurrent Three-Phase Fluidized Bed, Part 1," ORNL/MIT-209 (1975).

2. Burck, G.M., K. Kodama, R.G. Markeloff, and S.R. Wilson, "Cocurrent Three-Phase Fluidized Bed, Part II," ORNL/MIT-213 (1975).

3. Østergaard, K., "Three-Phase Fluidization," Chapt. 18 in Fluidization, Davidson and Harrison, eds., pp. 752-780, Acadamic Press, New York (1971).

4. Scott, C.D., and C.W. Hancher, "Use of a Tapered Fluidized Bed as a Continuous Bioreactor," ORNL.

SATISFACTION GUARANTEED

NTIS strives to provide quality products, reliable service, and fast delivery. Please contact us for a replacement within 30 days if the item you receive is defective or if we have made an error in filling your order.

▶E-mail: info@ntis.gov
▶Phone: 1-888-584-8332 or (703)605-6050

Reproduced by NTIS

National Technical Information Service
Springfield, VA 22161

This report was printed specifically for your order from nearly 3 million titles available in our collection.

For economy and efficiency, NTIS does not maintain stock of its vast collection of technical reports. Rather, most documents are custom reproduced for each order. Documents that are not in electronic format are reproduced from master archival copies and are the best possible reproductions available.

Occasionally, older master materials may reproduce portions of documents that are not fully legible. If you have questions concerning this document or any order you have placed with NTIS, please call our Customer Service Department at (703) 605-6050.

About NTIS

NTIS collects scientific, technical, engineering, and related business information – then organizes, maintains, and disseminates that information in a variety of formats – including electronic download, online access, CD-ROM, magnetic tape, diskette, multimedia, microfiche and paper.

The NTIS collection of nearly 3 million titles includes reports describing research conducted or sponsored by federal agencies and their contractors; statistical and business information; U.S. military publications; multimedia training products; computer software and electronic databases developed by federal agencies; and technical reports prepared by research organizations worldwide.

For more information about NTIS, visit our Web site at **http://www.ntis.gov**.

NTIS

Ensuring Permanent, Easy Access to U.S. Government Information Assets

U.S. DEPARTMENT OF COMMERCE
Technology Administration
National Technical Information Service
Springfield, VA 22161 (703) 605-6000